Tension of Membranes Expressing the Hemagglutinin of Influenza Virus Inhibits Fusion

Ruben M. Markosyan, Grigory B. Melikyan, and Fredric S. Cohen
Rush Medical College, Department of Molecular Biophysics and Physiology, Chicago, Illinois 60612 USA

ABSTRACT The effects of membrane tension on fusion between cells expressing the hemagglutinin (HA) of influenza virus and red blood cells were studied by capacitance measurements. Inflation of an HA-expressing cell was achieved by applying a positive hydrostatic pressure to its interior through a patch-clamp pipette in the whole-cell configuration. Inflating cells to the maximum extent possible without lysis created a membrane tension and completely inhibited low-pH-induced fusion at room temperature. Fully inflated cells that were subsequently deflated to normal size resumed the ability to fuse in response to low pH. At the higher temperature of 32°C, fusion conditions were sufficiently optimal that full inflation did not hinder fusion, and once formed, pores enlarged more rapidly than those of never inflated cells. It is suggested that under fusogenic conditions HA causes the formation of a dimple within the membrane in which it resides, and that membrane tension hinders fusion by preventing the formation of dimples. Because dimpling bends the bilayer portion of bound membranes so that they come into intimate contact, the damping of dimpling would suppress this initial step in the fusion process.

INTRODUCTION

Membrane fusion is a ubiquitous event in cell biology, during which formerly distinct membranes merge and the two aqueous compartments become one through the action of fusion proteins. For fusion to occur membranes must first bind. But even after binding the membranes have not yet come into intimate (i.e., molecularly close) contact. In exocytotic systems, after triggering secretion, membranes that are already docked (bound) come into intimate contact by the local bending of the plasma membrane toward the granule membrane (Chandler and Heuser, 1980; Ornberg and Reese, 1981). This bending of the cell membrane is termed *dimpling*. In viral fusion, molecularly long distances between membranes must be reduced in the time between binding and fusion. In the specific case of fusion induced by the hemagglutinin (HA) of influenza virus, the membrane expressing HA and the target membrane are known to be separated in the bound state by the distance of the HA trimer, ~13.5 nm (Wilson et al., 1981). This appreciable distance must be reduced before the lipid rearrangements of fusion can proceed. It is not yet known whether the membranes come into local contact through dimple formation, as in exocytosis, or by wider contact, approaching each other along an extended interface. Local contact could be effected either by the creation of a dimple in only one of the two membranes, or by the creation of a dimple in both. The envelope of isolated influenza virus is known to deform at low pH (the trigger for fusion if bound to a target membrane), but whether these morphologically observed protrusions are related to fusion is not yet clear (Ruigrok et al., 1992; Shangguan et al., 1997). Complementary protrusions and pits on influenza virus and target liposome membranes have been detected by quick-freezing electron microscopy. This complementarity has been interpreted to result from dimples of apposing membranes touching (Kanaseki et al., 1997).

Because overall tension of a membrane should suppress dimple formation, ascertaining whether application of membrane tension to that membrane inhibits fusion should provide a means of determining whether dimple formation on a viral protein-containing membrane is critical for intimate contact (Kozlov and Chernomordik, 1998). A cell membrane can be stressed by applying a positive pressure to the interior of a patch pipette in the whole-cell configuration (Solsona et al., 1998). This procedure inflates cells, increasing the apparent diameter significantly. When a cell is maximally inflated, a tension should be generated.

Using this technique, the effect of tension on the fusion of intracellular granules to plasma membrane has been studied in mast cells. Exocytosis was blocked in fully inflated cells; it resumed after the inflation pressure was relieved and the cells were returned to their original sizes (Solsona et al., 1998). But because exocytosis is a complicated process requiring many steps that depend on a multitude of proteins and intracellular factors, it is difficult to determine whether tension per se was responsible for the blockage, or if the inhibition of degranulation resulted from a mechanism not directly related to fusion. For example, inflation could have caused secretory granules to move away from plasmalemma (Chandler et al., 1989; Solsona et al., 1998). On the other hand, the inhibition could have been caused by a mechanism directly related to fusion. For example, mechanical tension could have suppressed dimple formation (Solsona et al., 1998). Fusion in viral systems, however, is generally much simpler than in exocytosis: only one or two types of proteins are involved, and because fusion takes place outside the

Received for publication 8 March 1999 and in final form 5 May 1999.

Address reprint requests to Dr. Fred S. Cohen, Department of Physiology, Rush Medical College, 1653 West Congress Parkway, Chicago, IL 60612-3864. Tel.: 312-942-6753; Fax: 312-942-8711; E-mail: fcohen@rush.edu.

0006-3495/99/08/943/10 $2.00

cell, complex cytosolic interactions should not significantly affect the fusion process.

In this work we investigated whether bending of a HA-expressing membrane into a dimple is required for fusion to a target membrane. We found that inflating HA-expressing cells inhibited fusion to erythrocytes. We argue that this inhibition was caused by membrane tension generated by inflation and that the specific inhibitory factor was the prevention of dimpling of the HA-containing membrane toward the target membrane.

MATERIALS AND METHODS

Cell maintenance and treatment

GP4f and HAb2 cell lines (National Institutes of Health (NIH) 3T3 fibroblasts constitutively expressing the A/Japan/57/305 strain of influenza hemagglutinin; Doxsey et al., 1985) were grown in Dulbecco's minimum essential medium (GIBCO BRL, Gaithersburg, MD) supplemented with 10% Cosmic Calf serum (HighClone Laboratories, Logan, UT). HA300a cells (Chinese hamster ovary cells stably transfected with X:31 HA) were maintained in glutamine-deficient medium in the presence of 0.4 mM L-methionine sulfoximine (Sigma Chemical Co., St. Louis, MO) as described (Kemble et al., 1993). The cell lines were a generous gift from Dr. J. White (University of Virginia, Charlottesville). For patch-clamp experiments, cells were harvested by a brief incubation with trypsin/EDTA solution (Gibco BRL), transferred into regular growth medium, and plated onto a no. 1.5 coverglass placed in a 35-mm culture dish. Cells were incubated in complete medium for 35 min at 37°C, washed twice with PBS^{++} (PBS with Ca^{2+} and Mg^{2+}), and incubated with 0.2 mg/ml neuraminidase from *Clostridium perfringence* and 5 μg/ml L-1-tosylamide-2-phenylethyl-chloromethyl ketone-treated trypsin (both purchased from Sigma) for 10 min at room temperature. Trypsin was quenched by adding an excess of growth medium, and cells were washed twice with PBS^{++} and allowed to bind RBCs by incubating for 6–10 min with 1 ml of a 0.01% suspension in PBS^{++}. Unbound RBCs were removed by rinsing three times with PBS^{++}. The coverglass with cells was broken into small pieces, placed on ice, and used for patch-clamp experiment within 6 h.

Labeling RBC and video microscopy

Freshly collected human red blood cells (Rush Blood Gas Laboratory) were labeled with octadecylrhodamine B (R18; Molecular Probes, Eugene, OR) as described (Melikyan et al., 1995b), except that a lower concentration of membrane dye was used: 2.5 μg R18/5 ml of a 1% RBC suspension. Labeled RBCs were used for experiments within 2–3 days after labeling. Redistribution of R18 between an RBC and a HA-expressing cell was monitored with a 40× phase-contrast objective on an inverted microscope (Nikon Diaphot; Nikon Instrument Group) using a standard rhodamine filter cube (G2A; Nikon). Fluorescence was observed with an intensified CCD video camera (XR Gen III+; Stanford Photonics, Stanford, CA) and recorded with a super VHS videocassette recorder (SVO-500MD; Sony Corp., Park Ridge, NJ). Images were digitized with a frame grabber (Meteor; Matrox Electronic Systems, Dorval, QC, Canada) and a PC-based computer.

Electrophysiological measurements

Cells adhering to small pieces of coverglass were transferred into the patch chamber filled with a solution that contained (in mM) 150 *N*-methylglucamine aspartate, 5 $MgCl_2$, 2 Cs-HEPES (pH 7.2). Patch pipettes were filled with (in mM) 155 Cs glutamate, 5 $MgCl_2$, 5 1,2-bis(2-aminophenoxy)ethane-*N,N,N,N*-tetraacetic acid, and 10 Cs HEPES (pH 7.4). Measurements were conducted with an Axopatch 200A patch-clamp amplifier (Axon Instruments, Foster City, CA). The resistance of the patch pipettes was ~5 MΩ. After the whole-cell configuration was established, a cell-RBC pair was lifted from the bottom of the dish (Chernomordik et al., 1997). Fusion between a GP4f cell and RBC was triggered with a solution buffered to pH 4.8 with 20 mM Cs succinate. This low-pH solution was gently ejected from another micropipette, which was manipulated into close proximity to the cell-RBC pair. Fusion was monitored by changes in whole-cell admittance, using a software-based lock-in amplifier (Ratinov et al., 1998). In short, a computer-generated sine wave (200 Hz, ±25 mV peak to peak) was superimposed on a −40 mV holding potential and applied to the interior of the patch pipette. From the output signal of the patch-clamp amplifier, the in-phase and out-of-phase currents (with respect to applied voltage) and the DC currents were calculated on-line and stored to a hard disk. Fusion pore conductances were calculated off-line. The ensemble average of fusion pore conductance at a given condition was characterized by aligning all pore conductances at their moment of opening and determining the average conductance and standard error at every time point. Because the fusion pore conductance cannot be reliably calculated after full enlargement, the conductances of quickly growing pores were only determined at early times after opening. This would result in a drop in the sample size and underestimation of average pore conductances at longer times. To minimize this problem, when fusion pore conductances were too large to be unambiguously determined, they were assumed to maintain their last reliably calculated conductance value.

Cell inflation and temperature control

The temperature of the bathing solution was maintained either at room temperature (22–23°C) or at 32°C with a temperature controller (20/20 Technology, Wilmington, NC). A cell was inflated by applying a positive pressure of 10–28 cm of water to the interior of the patch pipette. The pressure was generated by forced air and controlled and monitored by an air-pressure manometer (Magnehelic; Dwyer Instruments, Michigan City, IN). The pressure required to fully inflate a cell depended on the cell line and varied from day to day but was relatively constant between cells on a given day. The total capacitance of a cell was measured by compensating the current transients in response to small command voltage steps, using the C-slow and series resistance (R_S) compensation circuitry of the patch-clamp amplifier. The reading of C-slow compensation was taken as the total cell capacitance. For the range of series resistance and capacitance of our experiments, this procedure was reasonably accurate, as verified by using an equivalent circuit. To determine the apparent membrane area, linear distances were measured from the screen of the video monitor and were converted into cell diameter, using a conversion factor that was obtained by calibration against a hemocytometer.

RESULTS

Inflation of cells resulted in significant increases of cell diameters without changes in membrane capacitance

We inflated GP4f and HAb2 cells (NIH 3T3 fibroblasts) as well as HA300a (Chinese hamster ovary, CHO) cells. The three are HA-expressing cell lines. All three types were slowly inflated to about three to four times their original volume by applying a pressure to the interior of the patch pipette. This internal pressure on the cell was increased in several steps. At each step, we waited for the cell to reach its new diameter before further increasing the pressure. The final pressure range varied from day to day, from 10 to 28 cm of water, but for the same batch of cells on the same day, the maximum pressure was similar for almost all cells,

varying by only ~25%. The final pressure range of 10–28 cm of water without lysing the cells was similar to that required to fully inflate mast and chromaffin cells (Solsona et al., 1998). Typically it took several minutes for an HA-expressing cell to inflate to the point at which the cell diameter did not increase further as the pressure was elevated (Fig. 1). Continuing to slightly elevate pressure beyond this point caused the cell to visually lose contrast and become almost transparent without appreciable increases in membrane conductance. We define such cells as "fully inflated." (The absence of conductance increases after inflation shows that significant numbers of stretch-activated channels were not opened. Similarly, conductance increases were not observed for fully inflated mast and chromaffin cells (Solsona et al., 1998).) When a cell reached the point of full inflation, any further increases in the inflation pressure inevitably resulted in cell damage, observed as a significant increase in current. The onset of visual transparency provided the marker that maximum pressure without rupture has been reached. The whole-cell capacitance of GP4f, HAb2, and HA300a cells did not significantly change with inflation (Table 1). Thus, inflation did not cause incorporation of new membrane into the cell membrane (e.g., via exocytosis). The increases in cell diameter without significant changes in total cell capacitance reduced the apparent specific capacitance by approximately twofold for GP4f and HAb2 cells (Table 1). However, even these reduced values of specific capacitance were somewhat higher than those reported for mast and chromaffin cells (Solsona et al., 1998). These capacitances indicate that the GP4f and HAb2 cells never reached the point of full spherical geometry: some infoldings probably remained, even at maximum inflation. In contrast, the apparent size of HA300a cells increased to a greater extent, ~2.5-fold in area, and hence their final specific capacitance was correspondingly lower.

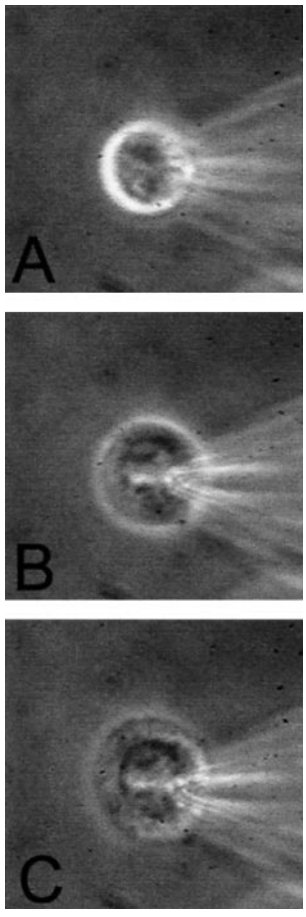

FIGURE 1 Inflation of a GP4f cell in whole-cell patch-clamp mode. A cell is shown before inflation (*A*), after partial inflation (*B*), and after full inflation (*C*). At full inflation, the cell has lost contrast. The image in *C* was taken after the maximum positive pressure of 12 cm of water had been applied to the interior of the patch pipette for 5 min at room temperature.

Inflation of GP4f cells does not affect the kinetics of fusion pore formation but promotes pore enlargement at 32°C

GP4f cells with one adhered RBC were selected for fusion experiments. After the whole-cell configuration was established, the cell-RBC complex was lifted off the dish. Lifting promoted isotropic inflation when pressure was applied; lifting also minimized problems that could have arisen from drift of the micromanipulator. Fusion was triggered by locally perfusing cells with a pH 4.8 solution ejected from a pipette for ~3 min at 32°C. After perfusion ceased, the solution surrounding the cell returned to the neutral pH of the bulk solution within several seconds (data not shown). In control experiments, the same procedures were followed, but with cells that had not been inflated. For control cells, a fusion pore typically opened within 1 min after the low-pH pulse was initiated. The conductance pattern of fusion pores between a GP4f cell and an RBC was the same as that previously observed by others (Spruce et al., 1991; Zimmerberg et al., 1994) (Fig. 2 *A*, *upper trace*): pore conductances exhibited quasi-stationary levels of ~0.5–1 nS that were sustained for ~20–30 s. To explore the effect of inflation on fusion, GP4f cells were inflated to their maximum diameter, and the pressure was held for ~3 min before pH was reduced. At 32°C, inflation caused a pore to grow much more rapidly than in the control experiments (Fig. 2 *A*, *lower trace*).

The traces of Fig. 2 *A* are representative, as can be seen by comparing them to the average conductance obtained by aligning individual records at the moment of pore opening and plotting the mean conductance as a function of time. At early times, the fusion pore conductances for control (uninflated) and inflated cells were indistinguishable (Fig. 2 *B*, *inset*). However, whereas a control pore did not usually grow beyond 1 nS for an extended period of time (Fig. 2 *B*, *filled circles*), the pore between a fully inflated cell and an RBC grew appreciably within 20 s. For inflated cells, ~2 s after opening a clear-cut breakthrough occurred in G_P.

We also compared the kinetics of fusion for control and inflated cells by plotting cumulative distributions of lag

TABLE 1 Specific membrane capacitance before and after inflation

Cell type	D_O/D_I (μm)	C_O/C_I (pF)	c_O/c_I (μF/cm^2)
GP4f (n = 14)	13.9 ± 0.5/19.3 ± 0.3	10.9 ± 0.8/10.8 ± 0.7	1.8 ± 0.2/0.92 ± 0.06
HAb2 (n = 8)	12.4 ± 0.7/18.4 ± 0.7	13.0 ± 1/12.8 ± 1	2.6 ± 0.2/1.2 ± 0.9
HA300a (n = 4)	11.8 ± 0.5/18.9 ± 0.4	7.2 ± 0.2/7.4 ± 0.2	1.6 ± 0.2/0.66 ± 0.02

The initial apparent cell diameter (D_O), total cell capacitance (C_O), and specific cell capacitance (c_O) are compared to their values at full inflation (D_I, C_I, c_I).

times between the application of low pH and fusion pore formation (Fig. 3 *A*). At 32°C, inflation did not affect the kinetics of fusion: it thus appears that the tension imposed on the cell membrane as a result of inflation has no effect on the formation of the fusion pore, but promotes pore enlargement after it has opened.

At room temperature, full inflation of an HA-expressing cell inhibits pore formation but still promotes pore enlargement

The inability of membrane tension to inhibit fusion at an elevated temperature (i.e., 32°C) might result if a sufficiently large percentage of HA were activated to overcome the tendency of tension to inhibit fusion. In principle, if tension could have been increased indefinitely, a value might have been reached that would inhibit fusion. But in practice, inflation, and thereby tension, could not be increased further without lysing the cell. Thus we made the conditions for fusion less optimal by lowering the system to room temperature (~23°C). When cells were inflated at room temperature, fusion pores did not occur for as long as 12 min after the pH was reduced in all 10 experiments attempted (Fig. 4 *B*). On the other hand, at room temperature control cells almost never failed to fuse: initial conductance was ~0.4 nS and remained within a limited range

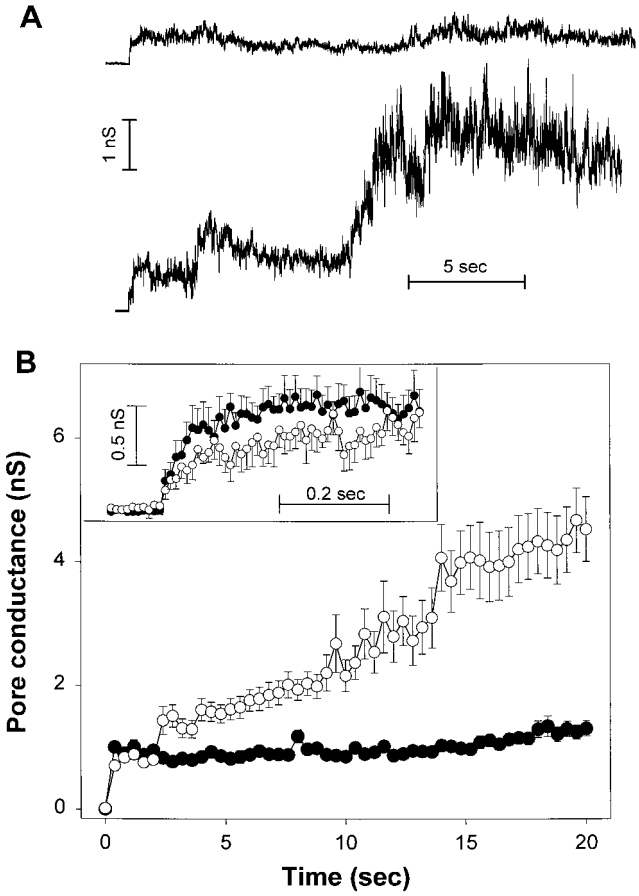

FIGURE 2 Representative records (*A*) and average profiles (*B*) of conductances of fusion pores between RBC and GP4f cells at 32°C. (*A*) Pore evolution for a control cell (*top trace*) and for a fully inflated cell (*bottom trace*). (*B*) Average conductance profiles for control (●, n = 11) and fully inflated (○, n = 13) cells. (*Inset*) The initial average conductances of fusion pores.

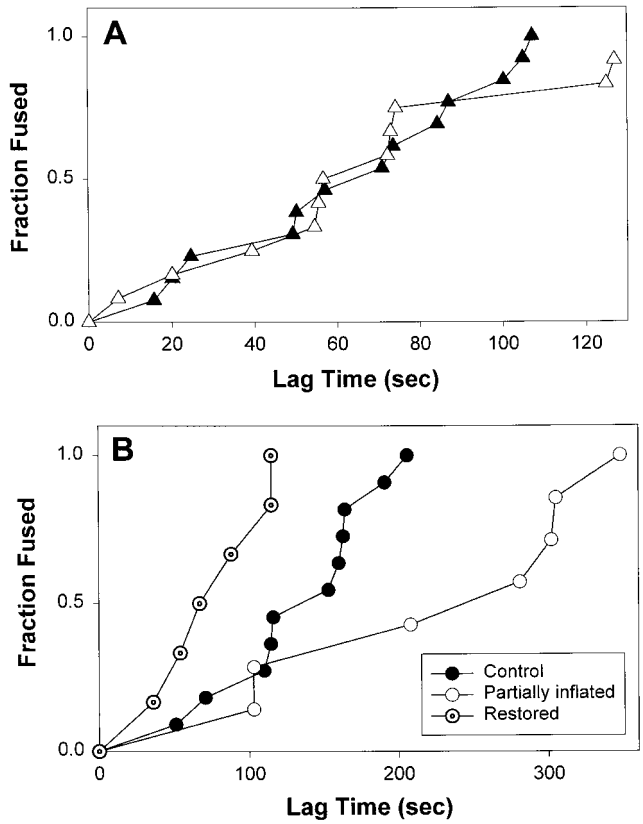

FIGURE 3 Kinetics of fusion of RBCs to GP4f cells. (*A*) Kinetics of fusion pore formation at 32°C for fully inflated (▲) and control (△) cells are shown as normalized cumulative distributions of the lag times between the reduction of pH to 4.8 and the detection of a fusion pore. These distributions give the fraction of cells that fused as a function of time. (*B*) At room temperature, lag times until formation of a fusion pore were longer for partially inflated (○) than for control (●) cells, which in turn were longer than for restored cells (⊙).

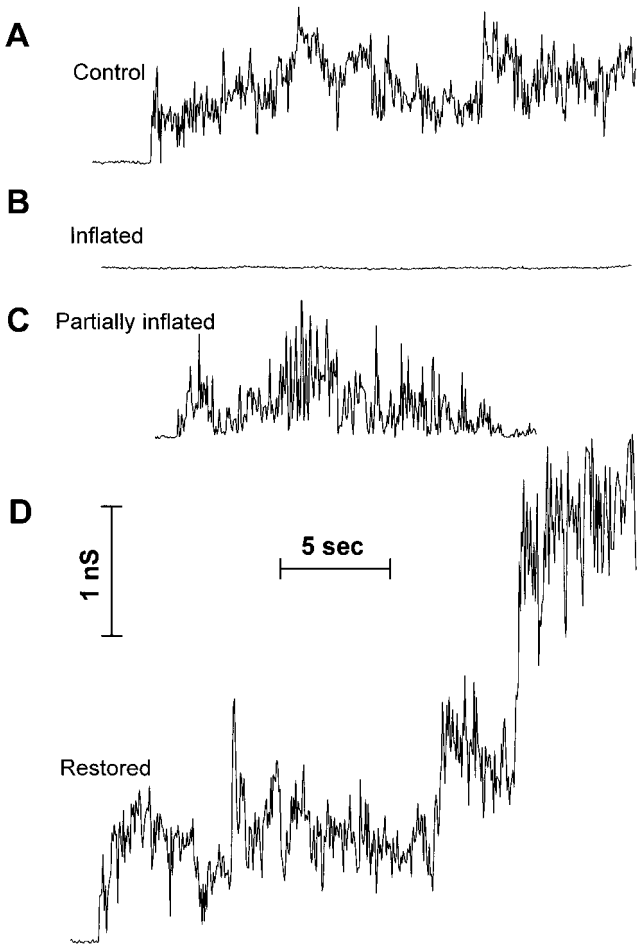

FIGURE 4 Representative examples of fusion pore evolution between GP4f cells and RBCs at room temperature. (*A*) Fusion pore conductance for a control cell. (*B*) Full inflation prevented the formation of pores. The illustrated record is at 9 min after pH reduction, with the in-phase component of the cell admittance shown. (*C*) For partially inflated cells, pores did not enlarge well, tending to exhibit rapid flicker and sometimes closing for an extended time. (*D*) Fusion pores of restored cells tended to enlarge better than those of control cells.

below 1 nS for a couple of minutes (Fig. 4 *A*). Inflation of GP4f cells inhibited not only pore formation, but lipid mixing as well: we did not observe any redistribution of membrane dye, R18, from an RBC to an inflated GP4f cell, whereas R18 transferred very efficiently after fusion pore opening in control experiments (data not shown). Furthermore, inflated cells with as many as three bound RBCs also did not show any sign of pore formation or lipid dye spread. Thus at room temperature inflation prevented even hemifusion for GP4f cells.

Next, we tested whether fusion could be observed when HA-expressing cells were somewhat less inflated. After determining the maximum pressure required to fully inflate cells on that day, GP4f cells were inflated by 60–80% of this pressure. The cell diameters increased, but the cells did not become transparent. These cells, referred to as "partially inflated," were capable of fusing to RBCs at room temperature after the pH was lowered to 4.8. However, the kinetics of fusion pore opening for partially inflated cells was statistically slower than for control cells (Fig. 3 *B*, *open and filled circles*, respectively). Surprisingly, partial inflation of GP4f cells led to formation of fusion pores that tended to flicker (Fig. 4 *C*), and the pores did not enlarge for several minutes after opening. This flickering led to an average fusion pore conductance of partially inflated cells (Fig. 5, *open circles*) that was significantly less than for control cells (*filled circles*).

The finding that partial inflation led to a reduced propensity for pore enlargement was not expected, and the basis for this phenomenon remains unclear. We therefore tested whether after formation of this small flickering pore between a partially inflated GP4f cell and RBC, an increase in pressure to its maximum value caused pore enlargement. When the pressure was increased in a single step to the maximum level, cells increased in diameter. This full inflation resulted in permanent opening and enlargement of the formerly small, flickering fusion pores (Fig. 6 *A*; the incre-

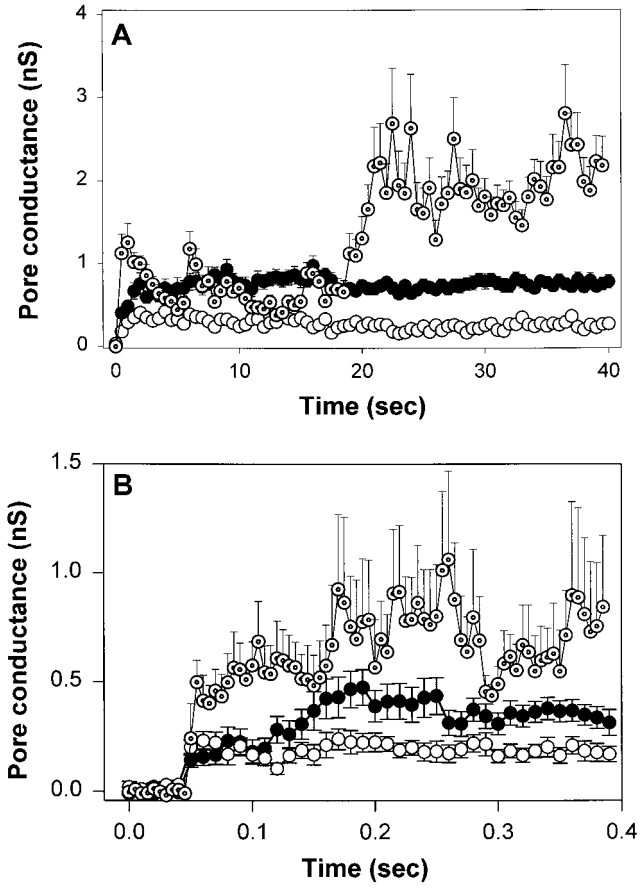

FIGURE 5 Average pore conductance profiles between an RBC and a GP4f cell under varied inflations. (*A*) The average conductance of a control pore (●, $n = 13$) was greater than for partially inflated cells (○, $n = 5$) because of the extensive flickering of the latter pores. For restored cells, pores had a greater tendency to grow (⊙, $n = 6$). Data points are decimated to aid visual clarity. (*B*) The data of *A*, plotted for the first 0.4 s after pore opening. The initial conductances of all three types of pores are similar, but pores of restored cells quickly grew. The time interval between points is 5 ms.

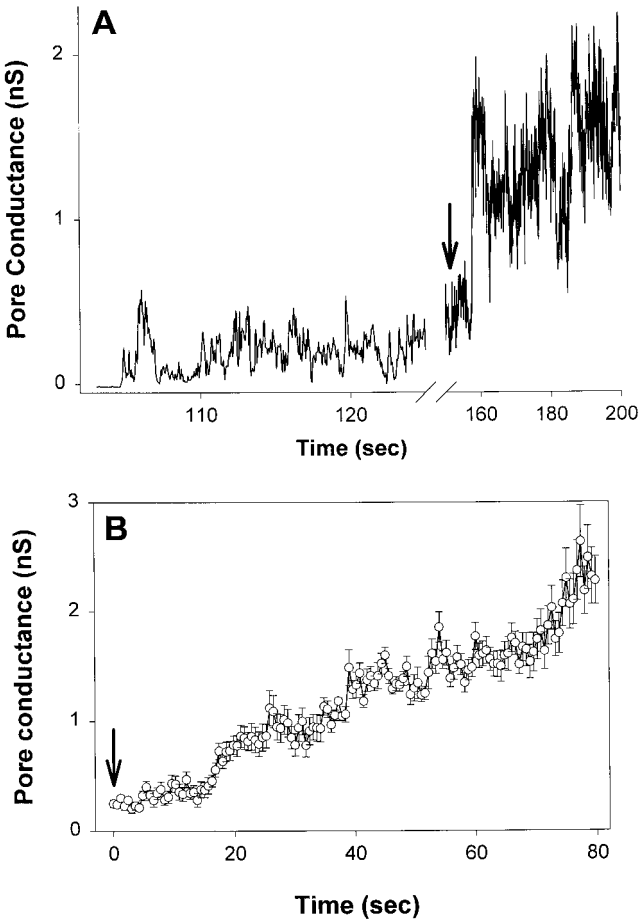

FIGURE 6 The effect of a pressure step on growth of a previously formed small flickering fusion pore between RBCs and partially inflated GP4f cells. (*A*) A representative experiment in which ~150 s after the small flickering pore was opened the pressure inside the patch pipette was elevated (*arrow*). The pore that had not enlarged for ~2.5 min increased its conductance soon after the inflating pressure was raised. (*B*) The average pore conductance profile built by aligning the small nonenlarging pores at the moment of the pressure increment (*arrow*, $n = 5$). The elevated pressure resulted in efficient dilation of fusion pores after a short delay, ~17 s.

ment in pressure is marked by an *arrow*). This was generally the case, as can be seen from the average conductance profile (Fig. 6 *B*), built by aligning already opened small pores at the moment the inflation pressure was increased to its final level (time = 0, marked by *arrows*, Fig. 6, *A* and *B*). On average, 17 s after the pressure was increased to fully inflate the cell, fusion pores began to grow, and they reached conductances of ~2–3 nS within a minute. (The pressure had to be applied slowly to noninflated cells to maintain pipette seals. As it took several minutes to fully inflate these cells after a pore formed and control pores tended to naturally enlarge during this lengthy time period, we could not definitively establish whether for control cells creating full inflation after pore formation caused these pores to better enlarge.) In short, full inflation of HA-expressing cells inhibits formation of fusion pores but promotes their enlargement once they have formed.

The kinetics of fusion pore formation and enlargement depends on a cell's inflation history

Breaking adhesions with the RBC by full inflation of the GP4f cell so that binding was no longer strong might have been the reason for the inhibition of fusion. To test this, a GP4f cell was inflated and then moved downward and pressed against a solitary RBC that was resting on the coverslip. The GP4f cell was then raised and the RBC rose with it, showing that good adhesion between the cells had been established. Binding was allowed to proceed for 3 min, after which lowering of pH did not lead to fusion. Thus the inhibition of fusion by full inflation did not depend on whether binding was established before or after cell inflation.

For fully inflated cells maintained at room temperature, the application of low pH (then returning to neutral pH) did not lead to fusion. We then explored whether these cells would fuse when the pressure was returned to normal. In the majority of experiments, the cell conductance increased (i.e., leaks developed) before the cell was adequately deflated. When the pressure was successfully removed, fusion pores sometimes formed and sometimes did not (i.e., pores were observed in four of 16 such experiments). These cells were maintained in their fully inflated state for 6 min after low pH was applied, and it took 5–8 min to deflate them. The reduced probability of fusion may have been caused by the inactivation, during this long time period, of some of the HA trimers that had previously been activated by low pH. But with a resumption of low pH for these deflated cells, pore formation was routinely observed (data not shown).

We tested whether the inhibition of fusion by the inflation process per se was reversible: that is, did inflation irreversibly alter something that affects fusion, other than membrane tension? Cells were maintained in a fully inflated state for ~4 min and then the pressure was relieved, without the pH ever being lowered. The cells were visually observed to deflate to their original sizes over a time course of several minutes. These cells are referred to as "restored." Restored cells could not be visually distinguished from control cells that had been patch clamped. A low pH pulse was then applied to a restored cell-RBC pair. In this case, pores formed with even faster kinetics (Fig. 3 *B*, *circles with dot*) and enlarged more efficiently (Figs. 4 *D* and 5 *A*) than for control cells (Fig. 5 *A*, *dotted and filled circles*, respectively). The initial conductances for control, partially inflated, and restored cells were similar (Fig. 5 *B*). Thus the propensity of a pore to form and enlarge, but not its initial conductance, was affected by the inflation protocols.

Pores formed by control and partially inflated cells reached semistable conductance levels below 1 nS. Pores between restored cells and RBCs enlarged more readily, reaching the conductance range of 2–3 nS within 30 s (Fig. 5 *A*). As restored cells should not have membrane tension, some persistent or even irreversible change has occurred in those cells; possibly the tension caused a dissociation or other changes in cytoskeletal elements.

DISCUSSION

Cell inflation causes membrane infoldings to stretch out and creates a membrane tension

Mammalian cell membranes usually have extensive infoldings; this results in an excess of membrane surface area with respect to volume. The apparent initial specific capacitances of GP4f and HAb2 (fibroblasts) cells were relatively high (1.8 and 2.6 $\mu F/cm^2$, respectively; Table 1), in agreement with values reported by others for fibroblasts ($\sim 2\ \mu F/cm^2$; Asami et al., 1990; Sukhorukov et al., 1993). Full inflation reduced the apparent specific capacitances by about twofold. But even these reduced values are considerably higher than the 0.5 $\mu F/cm^2$ reported by Solsona et al. (1998) for inflated mast and chromaffin cells. It has been reported that fibroblasts can lyse under hypotonic conditions without appreciable swelling (Sukhorukov et al., 1993). Perhaps the fibroblast membrane remains attached to the cell cortex at some loci. Our higher values of the specific capacitance after full inflation of the GP4f and HAb2 cells may be due to incomplete unfolding of the plasma membranes. The specific capacitance of fully inflated CHO cells (0.66 $\mu F/cm^2$) expressing HA (i.e., HA300a cells) was significantly smaller.

Because of normal infoldings, uninflated cells should not be under a Laplace tension. But interactions with cytoskeleton lead to small membrane tension, on the order of 0.01 mN/m (Hochmuth et al., 1996; Dai et al., 1998). The secretory granule membrane, which does not have infoldings, is, apparently, under considerably greater tension (Monck et al., 1990). Previous attempts to create tension over an entire plasma membrane have been made through the use of osmotic swelling. In swelling-induced exocytosis, volume-activated ion channels were stimulated and calcium influx altered (Moser et al., 1995). Thus swelling induced multiple phenomena. Furthermore, swelling of granules occured after fusion pore formation, independently of the osmotic state of the cell (Zimmerberg et al., 1987; Breckenridge and Almers, 1987). The osmotic conditions affected dispersal on vesicular contents after fusion pore formation (Curran and Brodwick, 1991; Fernandez et al., 1991; Borges et al., 1997). As swelling induces so many changes that are of direct consequence to secretion, it would be difficult to use this procedure to assess the effect of membrane tension on exocytosis.

The method of cell inflation introduced by Solsona et al. (1998) applies a maintained hydrostatic pressure to the cell interior and stretches out cell infoldings (as demonstrated by the increase in the cell's diameter). This method should thereby create membrane tension. A force exerted by the applied hydrostatic pressure should be distributed between the membrane itself, the cytoskeletal network, and the extracellular matrix. Cell-attached patch-clamp experiments have indicated that pulling plasma membrane into the pipette creates tension within the phospholipid bilayer portion of the membrane itself—i.e., the cytoskeleton and extracellular matrix do not support the entire tension (Akinlaja and Sachs, 1998). Full inflation should therefore create a significant membrane tension. In fact, further increases in inflation pressure inevitably resulted in cell lysis, strongly indicating that a tension had been generated. The promotion of pore enlargement by full inflation (Figs. 2 and 6) would naturally be accounted for by the generation of membrane tension.

Bilayer membranes can sustain tensions up to 3–4 mN/m before rupture (Kwok and Evans, 1981). Cell membranes can tolerate higher tensions than bilayers because their cytoskeleton as well as their membrane supports the tension. RBCs, for example, have rupture tensions of 10–12 mN/m (Evans et al., 1976). According to Laplace's law, applying a pressure of 20–24 cm of water ($2–2.4 \times 10^4\ N/m^2$) to a cell of radius 10 μm leads to a tension of 10–12 mN/m, in reasonable accord with the 10–28 cm of water that had to be applied to achieve maximum inflation of the HA-expressing cells.

Membrane tension can inhibit fusion

Full inflation of GP4f cells clearly generates membrane tension and completely prevents fusion under suboptimal (i.e., at room temperature) conditions. Full inflation may also cause other cellular effects, such as altering the anchoring of the membrane to cytoskeleton. Restored (inflated, then deflated) cells fuse with even faster kinetics than control cells (Fig. 3 *B*). Thus whatever changes occur as a result of full inflation, in addition to generation of tension, seem to promote rather than inhibit fusion. The normal membrane-cytoskeleton interactions are not expected to be quickly reestablished upon deflation, but tension should be relieved. It is noteworthy that whereas the history of inflation affected formation and growth of fusion pores, it did not affect the initial pore conductance. These conductances were the same for control, partially inflated, restored, and fully inflated cells.

It is not clear whether partial inflation generates significant membrane tension. The impaired formation of fusion pores with partially inflated cells (Fig. 3) is consistent with the creation of tension. But flickering was unusually pronounced for partially inflated cells as compared to control cells (Fig. 4). If one expects that pores better enlarge as tension increases, the observed vigorous flickering would be unanticipated if partial inflation created tension. Membrane tension may affect the growth of fusion pores in more than one manner. Although we cannot definitively explain the increased flickering for partially inflated cells, it is possible that the net effect of pulling on membranes by tension may not always be to enlarge a pore, but in some cases to actually close it. When membranes form the walls of a tube, tension causes the tube to collapse and even fission into two separate membranes when the tube length is greater than its diameter (Melikyan et al., 1984). Tension might therefore cause a toroidal fusion pore (Razinkov et

al., 1998) to collapse or fission, which would be observed as flickering. Planar membranes are under tension, on the order of 1 mN/m, and flickering is more pronounced when HA-expressing cells are fused to planar membranes than to RBCs (Melikyan et al., 1995a). Fully inflated cells should have considerably higher tensions than partially inflated cells and planar bilayers. Large tensions may cause pore enlargement, whereas for smaller tensions a collapse of the pore wall and even fissioning may dominate.

It is unlikely that changes in the cytoskeleton accounted for the slower kinetics of partially inflated cells because control cells fused more slowly than restored cells (Fig. 3). Furthermore, the status of cytoskeleton is not expected to be critical in HA-mediated fusion: HA-containing liposomes (virosomes) devoid of cytoskeleton fuse to target membranes with virtually the same kinetics as intact virus (Stegmann et al., 1987). The presence of HA appears to be all that is required for fusion. It is therefore likely that partially inflated cells were under tension, but this has not been definitively proved. In summary, although inflation probably leads to multiple cellular consequences, its direct effect of generating tension must contribute to some extent to inhibition of fusion, and it may be the dominant cause. Furthermore, the flickering phenomenon for partially inflated cells dramatically illustrates that fusion pores are extremely dynamic structures. Partial inflation exposes their dynamic properties and demonstrates that the regulation of open fusion pores is complex.

Prevention of dimpling would account for inhibition of fusion by tension

Why would increased membrane tension retard fusion? Creating a tension within a plasma membrane should suppress its ability to dimple toward the RBC membrane before fusion (Fig. 7). Dimpling may be a crucial step in the fusion process: inward dimpling of a plasma membrane toward an adjacent secretory granule has been observed at early stages of exocytosis before fusion (Chandler and Heuser, 1980; Ornberg and Reese, 1981). Dimpling provides the means for plasma and secretory granule membranes to locally make the intimate contact that must precede the lipid rearrangements of fusion. If a dimple is created within the HA-expressing membrane, HA must somehow bend its own membrane (Fig. 7, *C* or *D*). Because tension inhibits fusion, we conclude that a dimple forms in the HA-expressing membrane. This rules out the possibility that only the target membrane bends (Fig. 7 *B*). It has not yet been explored whether a dimple must also form in the target (e.g., RBC) membrane (i.e., Fig. 7, *C* or *D*) for fusion to occur. To create this dimple, the fusion peptide of HA would have to insert into the target membrane and locally pull this membrane toward the HA-expressing membrane (Fig. 7 *C*). Because the fusion peptide of HA does insert into the target membrane before fusion (Stegmann et al., 1991), the target membrane may also dimple. A recent theoretical model of fusion shows that if each low-pH-activated HA trimer causes its own local membrane deformation, the work of bending within this membrane is reduced by multiple HA trimers associating into a ring and together buttressing a somewhat larger single dimple (Kozlov and Chernomordik, 1998). As membrane tension increases, the formation of the dimple would become less favorable.

The degree of expected inhibition of dimple formation can be approximated. To create a dimple, membrane area must increase or cell volume decrease (so that membrane area can remain constant). Because tension and pressure are related by Laplace's law, the work required to stretch the membrane against constant tension is the same as the work required to decrease cell volume against an applied hydro-

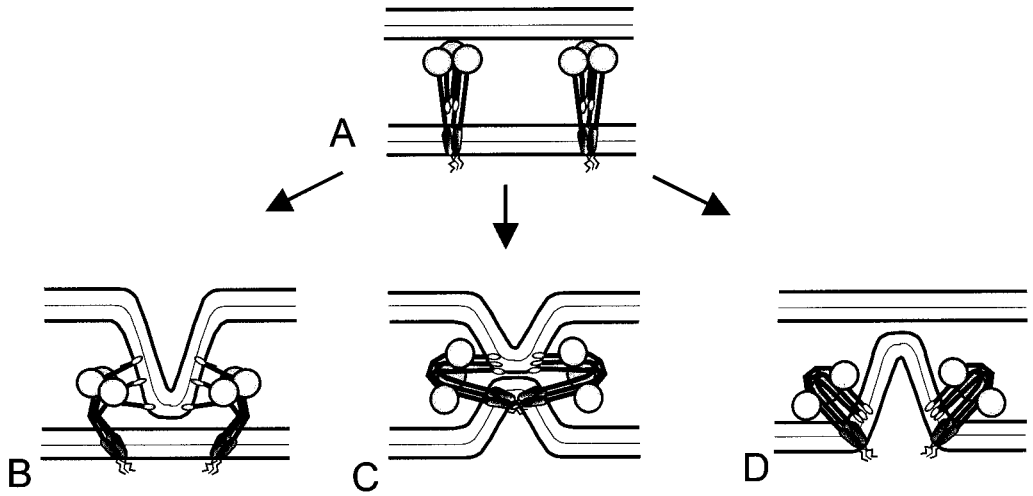

FIGURE 7 Possible origin of dimples involved in local membrane approach. (*A*) HA trimers induce initial binding at neutral pH. The membranes are still far apart. (*B, C, D*) At low pH, HA undergoes large-scale conformational changes and induces dimple formation. HA is depicted schematically; the distribution of inserted fusion peptide between the two membranes is not known. (*B*) HA induces a dimple in the target but not in the HA-expressing membrane. (*C*) HA induces dimpling in both membranes. (*D*) HA induces a dimple in only the HA-expressing membrane.

static pressure. About 75kT of additional work is required to create a dimple of radius 10 nm in a membrane under a tension of 1 mN/m, compared to the work required in the absence of tension. This would explain the inhibition of fusion by tension at room temperature. However, inflation did not inhibit fusion at 32°C. As several trimers are required for fusion, extents and rates of fusion are sensitive to the density of activated HA (Ellens et al., 1990; Melikyan et al., 1995a; Blumenthal et al., 1996; Danieli et al., 1996). Fusion is strongly dependent on temperature (Stegmann et al., 1991; Chernomordik et al., 1998): more HA trimers were probably activated at the higher temperature. It has been estimated that each additional activated HA trimer contributes 60kT to dimple formation (Kozlov and Chernomordik, 1998).

It has been proposed that lipid rearrangements at the site of a dimple lead to the formation of a stalk—the first merged structure (Leikin et al., 1987; Kozlov et al., 1989). The absence of R18 transfer from RBCs to GP4f cells that were fully inflated at room temperature (data not shown) indicates that the inhibition of fusion by tension occurred before stalk formation. Stalk formation has routinely been prevented by adding agents with positive spontaneous curvature, such as lysophosphatidylcholine (LPC). Thus, if tension inhibits the formation of dimples that are required for stalk formation, tension would be expected to inhibit fusion upstream of the LPC-arrested stage. This appears to be experimentally the case: if fusion conditions are established in the presence of LPC, fusion does not occur, but subsequent removal of LPC leads to fusion. (As with inhibition by tension, fusion conditions must be suboptimal to demonstrate inhibition by LPC.) In the case of HA-mediated fusion, HA is arrested in a state that ensures fusion—even when pH has been returned to neutral—once LPC is removed (Chernomordik et al., 1997). In contrast, relieving fully inflated cells of their tension (after fusion conditions had been established) did not reliably lead to a resumption of fusion. With tension present, it appears that the HA trimers activated by low pH go into configurations that do not reliably support fusion once the blocking tension has been removed. (When pH was again lowered after a cell was deflated, fusion pores formed. This is similar to the restoration of exocytosis when swollen cells were relieved of pressure in the presence of the secretion stimulus (Solsona et al., 1998). Therefore, it is likely that increased tension prevents fusion at a state upstream of the arresting action of LPC: HA should be committed to fusion if the LPC-arrested stage is reached before membrane tension can inhibit fusion. In summary, we conclude that membrane tension prevents dimple formation within the HA-expressing membrane, and dimples form at a stage intermediate between pH activation of HA and the occurrence of stalk formation that can be blocked by LPC.

We thank Ms. Sofya Brener for technical assistance, Dr. Judith White for supplying the HA-expressing cell lines, Dr. Michael Kozlov for useful discussions, and Dr. Leonid Chernomordik for a critical reading of the manuscript.

Supported by National Institutes of Health grants GM 27367 and GM 54787.

REFERENCES

Akinlaja, J., and F. Sachs. 1998. The breakdown of cell membranes by electrical and mechanical stress. *Biophys. J.* 75:247–254.

Asami, K., Y. Takahashi, and S. Takashima. 1990. Frequency domain analysis of membrane capacitance of cultured cells (HeLa and myeloma) using the micropipette technique. *Biophys. J.* 58:143–148.

Blumenthal, R., D. P. Sarkar, S. Durell, D. E. Howard, and S. J. Morris. 1996. Dilation of the influenza hemagglutinin fusion pore revealed by the kinetics of individual cell-cell fusion events. *J. Cell Biol.* 135:63–71.

Borges, R., E. R. Travis, S. E. Hochstetler, and R. M. Wightman. 1997. Effects of external osmotic pressure on vesicular secretion from bovine adrenal medullary cells. *J. Biol. Chem.* 272:8325–8331.

Breckenridge, L. J., and W. Almers. 1987. Final steps in exocytosis observed in a cell with giant secretory granules. *Proc. Natl. Acad. Sci. USA.* 84:1945–1949.

Chandler, D. E., and J. E. Heuser. 1980. Arrest of membrane fusion events in mast cells by quick-freezing. *J. Cell Biol.* 86:666–674.

Chandler, D. E., M. Whitaker, and J. Zimmerberg. 1989. High molecular weight polymers block cortical granule exocytosis in sea urchin eggs at the level of granule matrix disassembly. *J. Cell Biol.* 109:1269–1278.

Chernomordik, L. V., E. Leikina, V. Frolov, P. Bronk, and J. Zimmerberg. 1997. An early stage of membrane fusion mediated by the low pH conformation of influenza hemagglutinin depends upon membrane lipids. *J. Cell Biol.* 136:81–93.

Chernomordik, L. V., V. A. Frolov, E. Leikina, P. Bronk, and J. Zimmerberg. 1998. The pathway of membrane fusion catalyzed by influenza hemagglutinin: restriction of lipids, hemifusion, and lipidic fusion pore formation. *J. Cell Biol.* 140:1369–1382.

Curran, M. J., and M. S. Brodwick. 1991. Ionic control of the size of the vesicle matrix of beige mouse mast cells. *J. Gen. Physiol.* 98:771–790.

Dai, J., M. P. Sheetz, X. Wan, and C. E. Morris. 1998. Membrane tension in swelling and shrinking molluscan neurons. *J. Neurosci.* 18: 6681–6692.

Danieli, T., S. L. Pelletier, Y. I. Henis, and J. M. White. 1996. Membrane fusion mediated by the influenza virus hemagglutinin requires the concerted action of at least three hemagglutinin trimers. *J. Cell Biol.* 133:559–569.

Doxsey, S. J., J. Sambrook, A. Helenius, and J. White. 1985. An efficient method for introducing macromolecules into living cells. *J. Cell Biol.* 101:19–27.

Ellens, H., J. Bentz, D. Mason, F. Zhang, and J. M. White. 1990. Fusion of influenza hemagglutinin-expressing fibroblasts with glycophorin-bearing liposomes: role of hemagglutinin surface density. *Biochemistry.* 29:9697–9707.

Evans, E. A., R. Waugh, and L. Melnik. 1976. Elastic area compressibility modulus of red cell membrane. *Biophys. J.* 16:585–595.

Fernandez, J. M., M. Villalon, and P. Verdugo. 1991. Reversible condensation of mast cell secretory products in vitro. *Biophys. J.* 59:1022–1027.

Hochmuth, R. M., J.-Y. Shao, J. Dai, and M. P. Sheetz. 1996. Deformation and flow of membrane into tethers extracted from neuronal growth cones. *Biophys. J.* 70:358–369.

Kanaseki, T., K. Kawasaki, M. Murata, Y. Ikeuchi, and S. Ohnishi. 1997. Structural features of membrane fusion between influenza virus and liposome as revealed by quick-freezing electron microscopy. *J. Cell Biol.* 137:1041–1056.

Kemble, G. W., Y. I. Henis, and J. M. White. 1993. GPI- and transmembrane-anchored influenza hemagglutinin differ in structure and receptor binding activity. *J. Cell Biol.* 122:1253–1265.

Kozlov, M. M., and L. V. Chernomordik. 1998. A mechanism of protein-mediated fusion: coupling between refolding of the influenza hemagglutinin and lipid rearrangements. *Biophys. J.* 75:1384–1396.

Kozlov, M. M., S. L. Leikin, L. V. Chernomordik, V. S. Markin, and Yu. A. Chizmadzhev. 1989. Stalk mechanism of membrane fusion. *Eur. Biophys. J.* 17:121–129.

Kwok, R., and E. Evans. 1981. Thermoelasticity of large lecithin bilayer vesicles. *Biophys. J.* 35:637–652.

Leikin, S. L., M. M. Kozlov, L. V. Chernomordik, V. S. Markin, and Yu. A. Chizmadzhev. 1987. Membrane fusion: overcoming of the hydration barrier and local restructuring. *J. Theor. Biol.* 129:411–425.

Melikyan, G. B., M. M. Kozlov, L. V. Chernomordik, and V. S. Markin. 1984. Fission of the bilayer lipid tube. *Biochim. Biophys. Acta* 776: 169–175.

Melikyan, G. B., W. D. Niles, and F. S. Cohen. 1995a. The fusion kinetics of influenza hemagglutinin expressing cells to planar bilayer membranes is affected by HA density and host cell surface. *J. Gen. Physiol.* 106: 783–802.

Melikyan, G. B., J. M. White, and F. S. Cohen. 1995b. GPI-anchored influenza hemagglutinin induces hemifusion to both red blood cell and planar bilayer membranes. *J. Cell Biol.* 131:679–691.

Monck, J. R., G. A. de Toledo, and J. M. Fernandez. 1990. Tension in secretory granule membranes causes extensive membrane transfer through the exocytotic fusion pore. *Proc. Natl. Acad. Sci. USA.* 87: 7804–7808.

Moser, T., R. H. Chow, and E. Neher. 1995. Swelling-induced catecholamine secretion recorded from single chromaffin cells. *Pflügers Arch.* 431:196–203.

Ornberg, R. L., and T. S. Reese. 1981. Beginning of exocytosis captured by rapid-freezing of *Limulus* amebocytes. *J. Cell Biol.* 90:40–50.

Ratinov, V., I. Plonsky, and J. Zimmerberg. 1998. Fusion pore conductance: experimental approaches and theoretical algorithms. *Biophys. J.* 74:2374–2387.

Razinkov, V. I., G. B. Melikyan, R. M. Epand, R. F. Epand, and F. S. Cohen. 1998. Effects of spontaneous bilayer curvature on influenza virus-mediated fusion pores. *J. Gen. Physiol.* 112:409–422.

Ruigrok, R. W. H., E. A. Hewat, and R. H. Wade. 1992. Low pH deforms the influenza virus envelope. *J. Gen. Virol.* 73:995–998.

Shangguan, T., D. P. Siegel, J. D. Lear, P. H. Axelsen, and J. Bentz. 1997. Morphological changes and fusogenic activity of the influenza virus hemagglutinin. *Biophys. J.* 74:54–62.

Solsona, C., B. Innocenti, and J. M. Fernandez. 1998. Regulation of exocytotic fusion by cell inflation. *Biophys. J.* 74:1061–1073.

Spruce, A. E., A. Iwata, and W. Almers. 1991. The first milliseconds of the pore formed by a fusogenic viral envelope protein during membrane fusion. *Proc. Natl. Acad. Sci. USA.* 88:3623–3627.

Stegmann, T., J. M. Delfino, F. M. Richards, and A. Helenius. 1991. The HA2 subunit of influenza hemagglutinin inserts into the target membrane prior to fusion. *J. Biol. Chem.* 266:18404–18410.

Stegmann, T., H. W. M. Morselt, F. P. Booy, J. F. L. can Breeman, G. Scherphof, and J. Wilschut. 1987. Functional reconstitution of influenza virus envelope. *EMBO J.* 6:2651–2659.

Sukhorukov, V. L., W. M. Arnold, and U. Zimmermann. 1993. Hypotonically induced changes in the plasma membrane of cultured mammalian cells. *J. Membr. Biol.* 132:27–40.

Wilson, I. A., J. J. Skehel, and D. C. Wiley. 1981. Structure of the haemagglutinin membrane glycoprotein of influenza virus at 3 Å resolution. *Nature.* 289:366–373.

Zimmerberg, J., R. Blumenthal, D. P. Sarkar, M. Curran, and S. J. Morris. 1994. Restricted movement of lipid and aqueous dyes through pores formed by influenza hemagglutinin during cell fusion. *J. Cell Biol.* 127:1885–1894.

Zimmerberg, J., M. Curran, F. S. Cohen, and M. Brodwick. 1987. Simultaneous electrical and optical measurements show that membrane fusion precedes secretory granule swelling during exocytosis of beige mouse mast cells. *Proc. Natl. Acad. Sci. USA.* 84:1585–1589.